Polarized emission from KCl:Eu^{2+} single crystals

2000 J. Phys.: Condens. Matter 12 3485

(http://iopscience.iop.org/0953-8984/12/14/322)

J. Phys.: Condens. Matter **12** (2000) 3485–3495. Printed in the UK PII: S0953-8984(00)10205-X

Polarized emission from KCl:Eu^{2+} single crystals*

Jun-Gill Kang†§, Youngku Sohn†, Min-Kook Nah†, Youn-Doo Kim† and Elmer A Ogryzlo‡

† Department of Chemistry, Chungnam National University, Taejeon, 305-764, Korea
‡ Department of Chemistry, University of British Columbia, Vancouver, BC, V6T 1Z1 Canada

E-mail: jgkang@hanbat.chungnam.ac.kr

Received 8 November 1999

Abstract. The polarization emission spectrum and the angular dependence of polarization ratio of the blue emission from KCl:Eu^{2+} were investigated at 78.8 K. The polarized emission at 420 nm consisted of several components. The angular dependence of polarization ratio of each component is proportional to $\sin(2\alpha)$ or $-\cos(2\alpha)$, when the exciting light is polarized at α with respect to the z-axis for the [100]–[010] optical arrangement. The relaxed excited states (RESs) of Eu^{2+} responsible for the 420 nm emission are presented in terms of the adiabatic potential energy surface (APES), taking into account the Jahn–Teller effect (JTE) coupling to the E_g mode and the spin–orbit (SO) interaction. The charge-compensating cation vacancy (CCV, V_c^-) also causes an additive perturbation.

1. Introduction

Alkali halide phosphors activated with colour centres have been studied as spectroscopic host material (Fukuda 1970, Choi *et al* 1991, Kang *et al* 1994, 1995). Specially, alkali halides doped with divalent europium ions, Eu^{2+}, which emit bright blue luminescence (420 nm), are recognized as suitable candidates for the active media of broadly turnable solid-state lasers and dosimetric applications (Bron and Wagner 1966, Blasse 1973, Owen *et al* 1981, Aguirre de Cárcer *et al* 1988). Consequently, the spectroscopic properties of Eu^{2+} doped in fluorite-type crystals and alkali halide crystals have been examined comprehensively (Merkle and Bandyopadhyay 1989, Rubio 1991, Lawson and Payne 1993, Radhakrishnan and Selvasekarapandian 1994, Sosa *et al* 1995). Most Eu^{2+}-doped fluorite-type crystals and alkali halide crystals produce two absorption bands in the UV region. These are attributed to transitions from the ground state with the $4f^7$ electronic configuration to the $4f^65d$ excited states. The low-energy absorption band with a 'staircase' structure has been drawn special interest. A large number of studies on an electron paramagnetic (EPR) spectrum, ionic thermocurrent spectrum and two-photon absorption spectrum studies have been performed to better understand the energy-level structure of the $4f^65d$ configuration of Eu^{2+} in various crystals (many references in Rubio 1991). Eu^{2+}-doped fluorite and alkali halide crystals excited within the absorption bands produced only one broad emission band. Systematic investigation including measurements of photoluminescence and decay kinetics have also been performed to characterize the strong blue emission (Muñoz *et al* 1988, Sosa *et al* 1995). However, the relaxed

* Dedicated to the memory of Professor B S Park at Soonchun National University.
§ To whom all correspondence should be addressed.

0953-8984/00/143485+11$30.00

excited states (RESs) of the Eu^{2+} ion responsible for the blue emission have not been revealed. Mugeński and Nagirnyi (1994) suggested that the 420 nm emission from KCl:Eu^{2+} might be correlated with the tetragonal minima on the adiabatic potential energy surface (APES) of the relaxed T_{2g} states due to the dynamic Jahn–Teller effect (JTE).

This study was undertaken to investigate the polarization of the blue emission from Eu^{2+} in KCl single crystals in terms of the polarized emission spectrum and the angular dependence of polarization ratio. We found that the 420 nm emission from Eu^{2+} originates from various anisotropic emitting centres. A theoretical model for the 420 nm emission has been formulated in terms of the Jahn–Teller effect (JTE) and spin–orbit (SO) interaction. The charge-compensating cation vacancy (CCV or V_c^-) due to the substitution of divalent europium ions into the KCl lattice also causes an additional perturbation. In this paper, we clearly establish the presence of blue emission and present a comprehensive model for the RESs of Eu^{2+} ions in KCl.

2. Experiment

A thoroughly ground, well mixed mixture of KCl (99.99+%, Aldrich) and anhydrous $EuCl_2$ (99.9%, Strem) was transferred into a quartz ampoule. After flushing the sample with Ar gas (99.999%) a few times, it was sealed under high vacuum. Crystals were grown under vacuum using the vertical Bridgman method.

To measure the luminescence and excitation spectra, an appropriately sized sample was placed on the cold finger of an Oxford CF-1104 cryostat. Excited light from either an He–Cd laser or an Oriel 1000 W Xe arc lamp was passed through an Oriel MS257 monochromator and focused on the sample. The luminescence spectrum was measured at a 90° angle with an ARC 0.5 m Czerny–Turner monochromator equipped with a cooled Hamamatsu R-933-14 photomultiplier tube.

The polarization spectrum and angular dependence of the polarization ratio in the perpendicular geometry were both measured. For these measurements, the excitation light was linearly polarized using a Glan–Thomson prism polarizer in a rotable mount. An analyser, consisting of a Glan–Thomson polarizer and a quarter-wave plate, was used to observe the polarization of the emitted radiation. The angular dependence of the polarization ratio was measured using a combination of a polarizer and an analyser. When the polarizer is set at α and the analyser is set at β with respect to the z axis, the intensity of the emission from a linear oscillator is given by

$$I \propto (a_y \sin\alpha + a_z \cos\alpha)^2 (a_x \sin\beta + a_z \cos\beta)^2 \tag{1}$$

for the [100]–[010] optical geometry, where a_i is a component of the unit vector of the oscillator. For a given angle α of the polarizer, two emission intensities ($I_\parallel$, $I_\perp$) were recorded by setting the angle of the analyser parallel ($I_\parallel$) or perpendicular ($I_\perp$) to that of the polarizer. Details of the optical arrangements have been described elsewhere (Choi *et al* 1991).

3. Results

The UV–visible absorption spectrum of KCl:Eu^{2+} single crystals was measured at room temperature. As shown in figure 1, the two absorption bands appeared at 245 nm and 345 nm in the absorption spectrum. These two absorption bands are due to the $4f^7 \rightarrow 4f^6 5d$ transition of Eu^{2+}. The low-energy absorption band shows the characteristic 'staircase' structure that has been found in the optical spectrum of Eu^{2+} in various host crystals. The 'staircase' structure has been interpreted in the framework of a model that considers the electrostatic interaction

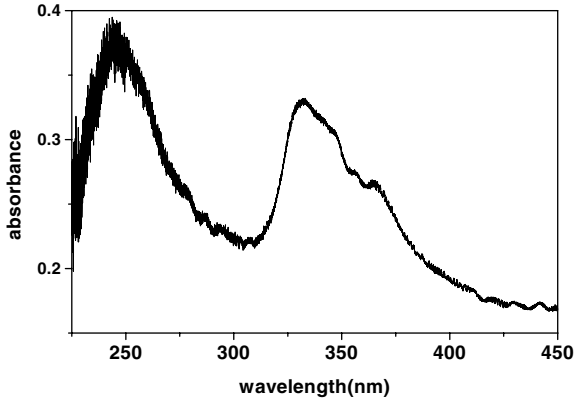

Figure 1. Absorption spectrum from KCl:Eu^{2+} measured at 78.8 K.

of the f and d electrons and the effect of the crystal field as zero-order perturbation (Merkle and Powell 1977, Rubio 1991). The effect of the f^6 electronic configuration is an additional perturbation. The electrostatic interaction between the f and d orbitals resulted in a set of spin octets and sextets for the $4f^65d$ excited state. Then, the crystal field splits these spin states into the octet state for the lower level and the sextet state for the higher level, and the separation of those levels increases with the crystal field strength. If the SO of $4f^6$ is comparable with the effect of the crystal field on the d orbital, it may give rise to seven states, $^7F_0$ through $^7F_6$, similar to the ground state of Eu^{3+}. The coupling of the octet state to the ^7F term may produce the 'staircase' structure in the low-energy absorption band. The 245 nm and 345 nm bands have been attributed to transitions from the ground $^8S_{7/2}$ state to the excited $E_g(4f^65d)$ and $T_{2g}(4f^65d)$ states, respectively.

The intensity spectrum of the emission from KCl: Eu^{2+} single crystals was measured at 78.8 K. As shown in figure 2(a), the single crystals under 325 nm excitation produced a very strong emission band peaking at 420 nm (hereafter, referred to as the A-band emission). The excitation spectrum of the A-band emission was also measured at $T = 78.8$ K. As shown in figure 2(b), a very weak band appeared at 260 nm and a strong band with a complicated structure appeared in the 310–410 nm region: the latter reflected the staircase feature. The excitation indicates that the A-band emission from KCl:Eu^{2+} is produced mainly by radiative decay from the T_{2g} level. Although the transition to the E_g level has a suitable oscillator strength compared with that to the lower level, most of the population of the E_g level may decay via a predominantly nonradiative process.

Intensity spectra of the A-band emission from Eu^{2+} in KCl polarized parallel and perpendicular to the direction of the electric vector of the exciting light were measured at 78.8 K. As shown in figure 3, the emission band polarized parallel (hereafter, referred to as A_Π) and perpendicularly (hereafter, referred to as A_Σ) are strikingly different. The difference between the A_Π and A_Σ intensities may be due to the different oscillators. This is unlike any previously reported emission spectra of Eu^{2+}-doped alkali halide single crystals, for which it was accepted that the spectrum consists of only one broad band in the well-quenched samples. The A_Π and A_Σ spectra resolve into at least four overlapping bands as shown in figure 4. The results of the spectrum resolution are summarized in table 1. Although the unpolarized A-emission band is not split, it may consists of two or more components, taking into account the polarized emission spectra. The unpolarized spectrum was also resolved using a Gaussian formula. The computer plot of a resolved spectrum and the experimental data of the corresponding emission spectrum

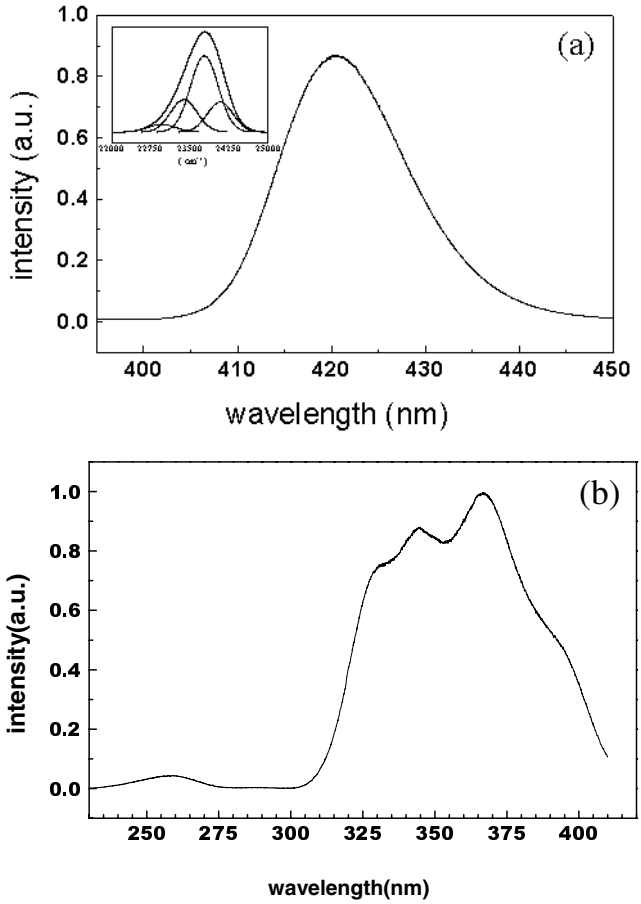

Figure 2. (a) Emission spectrum ($\lambda_{exc} = 325$ nm) and (b) excitation spectrum ($\lambda_{ems} = 420$ nm) from KCl:Eu^{2+} at $T = 78.8$ K.

Table 1. Results of spectrum resolution for the A_Π and A_Σ emission from KCl:Eu^{2+}. The exciting light was polarized along the [001] direction in the [100]–[010] optical arrangement.

	Component			
	1	2	3	4
Parallel				
peak position (nm)	22 878	23 299	23 751	24 118
% area	4.7	27.3	46.9	21.1
Perpendicular				
peak position (nm)	23 123	23 549	23 895	24 145
% area	15.5	37.7	34.3	11.2

with background subtracted are also shown in figure 2(a). The A-emission spectrum resolves into at least four overlapping bands. The results of the spectrum resolution are summarized in table 2.

The angular dependence of polarization ratio of each component in the A-band emission was measured in the perpendicular geometry at 78.8 K. Here, the intensity of component 1

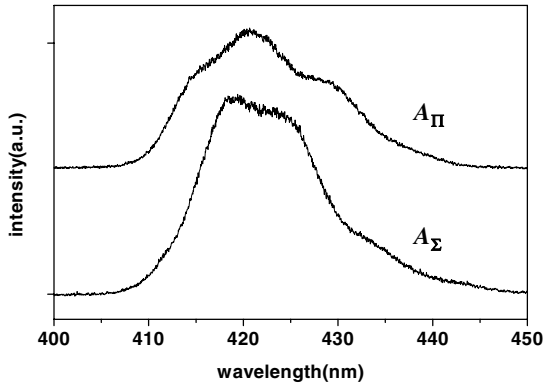

Figure 3. Polarized emission spectra from KCl:Eu^{2+}: top, the parallel polarized emission spectrum (A_Π) with both the polarizer and the analyser set at $\alpha = 0^\circ$ and $\beta = 0^\circ$ from the z axis, respectively, and bottom, the perpendicularly polarized emission spectrum (A_Σ) with polarizer and the analyser set at $\alpha = 0^\circ$ and $\beta = 90^\circ$, respectively ($T = 78.8$ K, $\lambda_{exc} = 366$ nm).

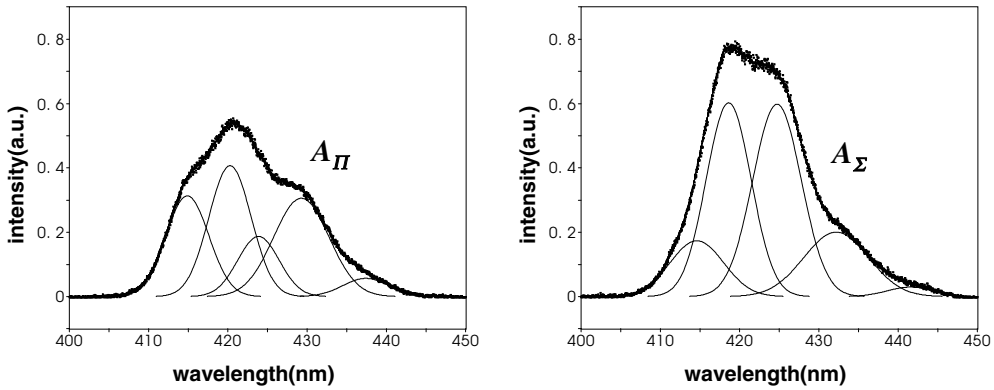

Figure 4. Resolution of the A_Π and A_Σ emission spectra from KCl:Eu^{2+} as the Gaussian formula.

Table 2. Results of spectrum resolution for the A-band emission from KCl:Eu^{2+}.

	Component			
	1	2	3	4
Peak position (cm^{-1})	22 955	23 379	23 771	24 075
% area	5.42	21.9	53.2	19.5
$P(\alpha) \propto$	—	$\sin(2\alpha)$	$-\cos(2\alpha)$	$\sin(2\alpha)$

(436 nm) is too weak to obtain the apparent $P(\alpha)$. The low-energy and high-energy sides were chosen for components 2 and 4, respectively, in order to reduce the overlapping with the strongest component 3. As shown in figure 5, components 2 (430 nm) and 4 (413 nm) show similar patterns for the angular dependence of polarization ratio. When the exciting light is polarized at $\alpha = 0^\circ$ or 90°, $P(\alpha)$ becomes 0. It is maximal at $\alpha = 45^\circ$ and minimal at $\alpha = 135^\circ$. The angular dependence of these bands is proportional to $\sin(2\alpha)$. On the other hand, the polarization ratio is proportional to $-\cos(2\alpha)$ for component 3 (420 nm). The polarization ratio $P(\alpha)$ is minimal at $\alpha = 0^\circ$ or 180° and maximal at $\alpha = 90^\circ$. At $\alpha = 45^\circ$ or

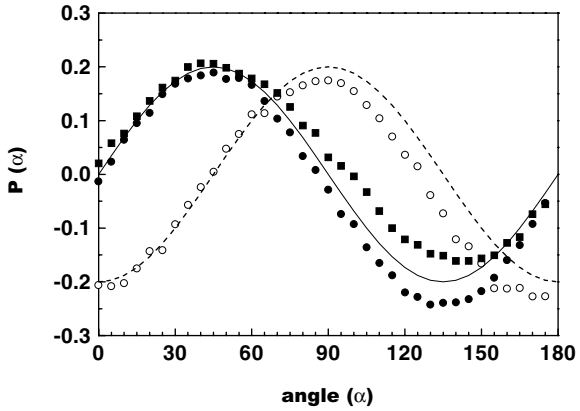

Figure 5. Angular dependence of polarization ratio of the 413 nm (■), 420 nm (○) and 430 nm (●) emission from KCl:Eu^{2+} in the perpendicular geometry ($T = 78.8$ K). The lines are calculated from: $P(\alpha) = 0.2\sin(2\alpha)$ (solid line) and $P(\alpha) = -0.2\cos(2\alpha)$ (broken line).

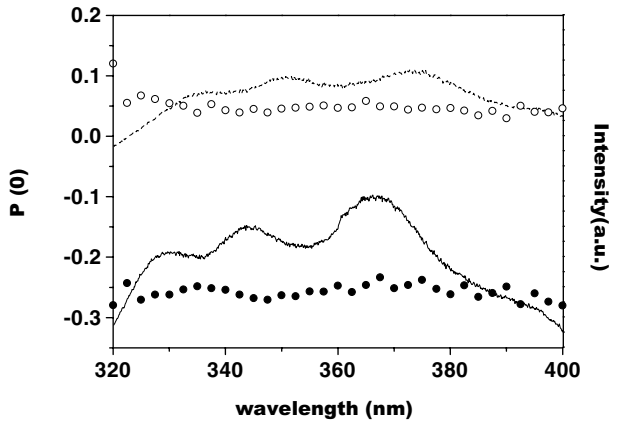

Figure 6. Polarization spectra of the 418 nm emission (solid circle and line) and the 430 nm emission (open circle and broken line) from KCl:Eu^{2+} ($T = 78.8$ K).

135°, the polarization ratio changes from negative to positive or vice versa. The polarization spectra of the A-band emission from KCl:Eu^{2+} were also measured at $T = 78.8$ K to reveal the nature of absorbing and emitting oscillators. As shown in figure 6, the excitation spectra of both A_Π and A_Σ do not differ and the sign of degree of polarization ratio does not change throughout the entire excitation wavelength region. This suggests that the absorbing oscillators for the A_Π and A_Σ are identical, but the emitting oscillators are different. Nonradiative transitions between the two emitting centres probably occur after the excitation.

The dependence of the polarization ratio on the angle of the exciting light suggests that the absorbing/emitting dipole should have a preferential orientation relative to the electric vector of the exciting light. The characteristic feature in the polarization of the A-band emission from KCl: Eu^{2+} could be associated with one of the following factors: (1) the aggregation of Eu^{2+} ions in KCl, (2) a charge compensating cation vacancy (CCV, V_c^-) and (3) the symmetry properties of the RESs of T_{2g}. The absorption and emission spectra of KCl:Eu^{2+} are reported to be sensitive to the precipitation state of Eu^{2+} ions in alkali halide matrix. A large number

of bands appeared in the low-temperature emission spectrum of well aged crystals at several annealing temperatures (Rubio 1991). In particular, four emission bands peaking at 410, 421, 439 and 478 nm were observed in the well aged KCl:Eu^{2+}. The dependence of these bands on the ageing time and the annealing temperature ascertained the assignments of those bands as a stable $EuCl_2$ centre (410 nm) dipoles and the first products of aggregation (421 nm), and a metastable $EuCl_2$-type precipitation (439 nm and 478 nm). We also investigated the emission spectra of KCl single crystals highly doped with Eu^{2+} or Eu^{3+} ions in KCl. The 410 and 478 nm bands were not present in the emission spectra of the as-grown samples, ruling out that the possibility of Eu^{2+} ion aggregation as the anisotropic centre in the A-band emission. Mugeński and Nagirnyi (1994) also suggested that the emission of aggregation products in KCl:Eu^{2+} is not polarized.

Next, let us consider the nature of the compensating cation vacancy (CCV). When divalent europium cation is incorporated into the KCl lattice by substitution; it could be associated with a CCV, which will affect the A-band emission. The nature of the perturbation depends on the location of the CCV with respect to the Eu^{2+} ion, i.e. whether it is the nearest neighbour (nn) or the next-nearest neighbour (nnn). Eu^{2+}–V_c^- complexes in the nn and nnn positions were proposed to explain the observed intensity ratios for the orthorhombic and axial EPR spectrum (Hernandez *et al* 1981). The intensity of the orthorhombic (nn) spectrum was found to be more abundant than that of the axial (nnn) spectrum. If the polarization of the A-band emission from KCl:Eu^{2+} is associated with anisotropy of the Eu^{2+}–V_c^- complex, it should be characterized by C_4 (nnn) or C_2 (nn) symmetry properties. According to the mathematical formulae of $P(\alpha)$ for three possible preferential orientations along the fourfold (C_4), threefold (C_3) and twofold (C_2) symmetry axes, listed in table 3, no formulae fit the observed $P(\alpha)$ proportional to $\sin(2\alpha)$ or $-\cos(2\alpha)$ for the components of the A-band emission in the [100]–[010] geometry. It indicates that although the interaction between Eu^{2+} cation and V_c^- is considered a static problem, the CCV is not strong enough to produce the principal anisotropic effect on the A-band emission. The observed unusual angular dependence of the polarization ratio could not be associated with a static distortion such as the CCV, but with a dynamic distortion such as the electron–lattice interaction. The tetragonal distortion due to the dynamic JTE has been ascribed to an isotropic effect on the A-band emission from KCl:Eu^{2+} by Mugeński and Nagirnyi (1994).

Table 3. Mathematical formulas for the polarization ratio in the [100]-[010] optical arrangement.

Symmetry axis	Electric dipole	$P(\alpha)$
C_4	$\pi \to \pi$	$\cos 2\alpha$
	$\pi \to \sigma$	$-\dfrac{\cos 2\alpha \cos^2 2\alpha}{1+\sin^2\alpha}$
	$\sigma \to \sigma$	$\dfrac{\cos 2\alpha \cos^2 \alpha}{2+\cos^2\alpha}$
C_3	$\pi \to \pi$	0
	$\pi \to \sigma$	0
	$\sigma \to \sigma$	0
C_2	$\pi \to \pi$	$\dfrac{\cos 2\alpha \cos^2 2\alpha}{2+\cos^2\alpha}$
	$\pi \to \sigma$	$-\dfrac{\cos 2\alpha \cos^2 2\alpha}{5+\sin^2\alpha}$
	$\sigma \to \sigma$	$\dfrac{\cos 2\alpha \cos^2 2\alpha}{10+\sin^2\alpha}$

4. Discussion

For Eu^{2+}, the interaction between the $4f^6$ electrons and the 5d electron causes a very complicated problem compared with the pure T_{2g} state arising from a single electron in the d orbital in the octahedral crystal-field potential. If the interaction is sufficiently strong, the states are strongly mixed and a large number of distinct optical transitions appear possible in the excitation or absorption spectra. For KCl: Eu^{2+}, however, two broad absorption bands are observed in the transition from the $^8S_{7/2}$ ground state to the split $4f^65d$ states. The structure of the ^7F_J states of the $4f^6$ electrons is superimposed on the low-energy absorption band. This indicates that the interaction between the $4f^6$ electrons and the 5d electron could be fairly weak. Otherwise, the electronic structures arising from the $4f^65d$ electronic configuration might be reflected as multiple absorption bands in the transition from the $^8S_{7/2}$ ground state to the split $4f^65d$ states. One of the characteristic features in the A-band emission from KCl:Eu^{2+} is seen in the band-width and the Stokes shift. The SO interaction of the $4f^N$ electronic configuration is exceptionally strong, compared with other configurations arisen from s, p or d electrons. The strong SO interaction may reduce the effect of the Jahn–Teller (JT) interaction, and the Stokes shift may be very small in the optical transition. For instance, the absorption and emission spectra responsible for the f $\rightarrow$ f transition consist of groups of sharp lines and the Stokes shift is negligible. Assuming that $E_{JT} = 1/2$ Stokes shift, the JT stabilization energy is $\sim$0.22 eV (1750 cm^{-1}) for the A-band emission from KCl:Eu^{2+}. The strong JT stabilization indicates that the contribution of the $4f^6$ electronic states to the A-band emission and the reduction of the JT effect (JTE) due to the SO interaction would be very small. Accordingly, we confined the relaxation process of the A-band emission to the problem with the t_{2g} states of the Eu^{2+} 5d orbital.

First, we shall find out what kind of minima would exist on the APES of the first excited T_{2g} state. Öpik and Pryce (1957) discussed the JTE in triply degenerate T_1 or T_2 states. Except for the ^1T state, the JT interaction with the $E_g(Q_2, Q_3)$ mode predominates over the coupling with the $T_{2g}(Q_4, Q_5, Q_6)$ mode. If the $T\otimes E_g$ vibronic problem is major, the JT and SO Hamiltonian for $^2T_{2g,yz}$, $^2T_{2g,zx}$ and $^2T_{2g,xy}$ in the spin $|m_s; \pm 1/2\rangle$ degeneracy is given by

$$\begin{vmatrix} -\frac{1}{2}b\left(Q_2 - \frac{Q_3}{\sqrt{3}}\right) - \varepsilon & \mp\frac{i\rho\lambda}{2} & \frac{\rho\lambda}{2} \\ \pm\frac{i\rho\lambda}{2} & \frac{1}{2}b\left(Q_2 + \frac{Q_3}{\sqrt{3}}\right) - \varepsilon & \mp\frac{i\rho\lambda}{2} \\ \frac{\rho\lambda}{2} & \pm\frac{i\rho\lambda}{2} & -\frac{b}{\sqrt{3}}Q_3 - \varepsilon \end{vmatrix} + \frac{K_E}{2}(Q_2^2 + Q_3^2)\bar{I} = 0 \qquad (2)$$

where b and K_E are the JT coupling constant and the force constant for the E_g modes, respectively, ρ is -1 for the d orbital, $\bar{I}$ is a three-dimensional unit matrix, and the last term is the lattice energy. Excluding off-diagonal SO elements, there are three tetragonal minima (hereafter, referred to as T) on the adiabatic potential energy surface (APES) in the (Q_2, Q_3) space. The positions of the three minima (T_{xy}, T_{yz}, T_{zx}) are given by the coordinates, $(0, Q_0/\sqrt{3})$, $(Q_0/2, -Q_0/2\sqrt{3})$ and $(-Q_0/2, -Q_0/2\sqrt{3})$, respectively, where $Q_0 = b/K_E$. For the $^2T_{2g}$ state, the off-diagonal SO terms may cause mixing of the three mutually orthogonal paraboloids, resulting in two kinds of minimum on each of paraboloid. An additional tetragonal minima (T^*_{xy}, T^*_{yz}, T^*_{zx}) can coexist at point $(0, -Q_0/2\sqrt{3})$, $(Q_0/2\sqrt{3}, Q_0/6)$ and $(-Q_0/2\sqrt{3}, Q_0/6)$, respectively, for suitable values of K_E, b and λ. To examine how mixing the states affected the depths of the minima, we calculated the cross section of the paraboloid with the T_{xy} minimum along the Q_3 axis. Choosing suitable values of A and b, the APES was computed for several values of $g(= \lambda/b)$. As shown in figure 7(a), when $g < 1$, the two kinds of stationary point, T_{xy} and T^*_{xy}, are not significantly affected by the SO. However, when $g \geqslant 1$, there is a significant change in the depth of the T^*_{xy} minimum. As λ increases, the T^*_{xy} minimum collapses

into a saddle point, while the T_{xy} minimum remains as a stationary point. Accordingly, two minima, T and T^*, can coexist on each of the $^2T_{2g}$ APESs, if the SO interaction is not much stronger than the JTE. The maps of two kinds of minimum on the $^2T_{2g}$ APES are shown in figure 7(b).

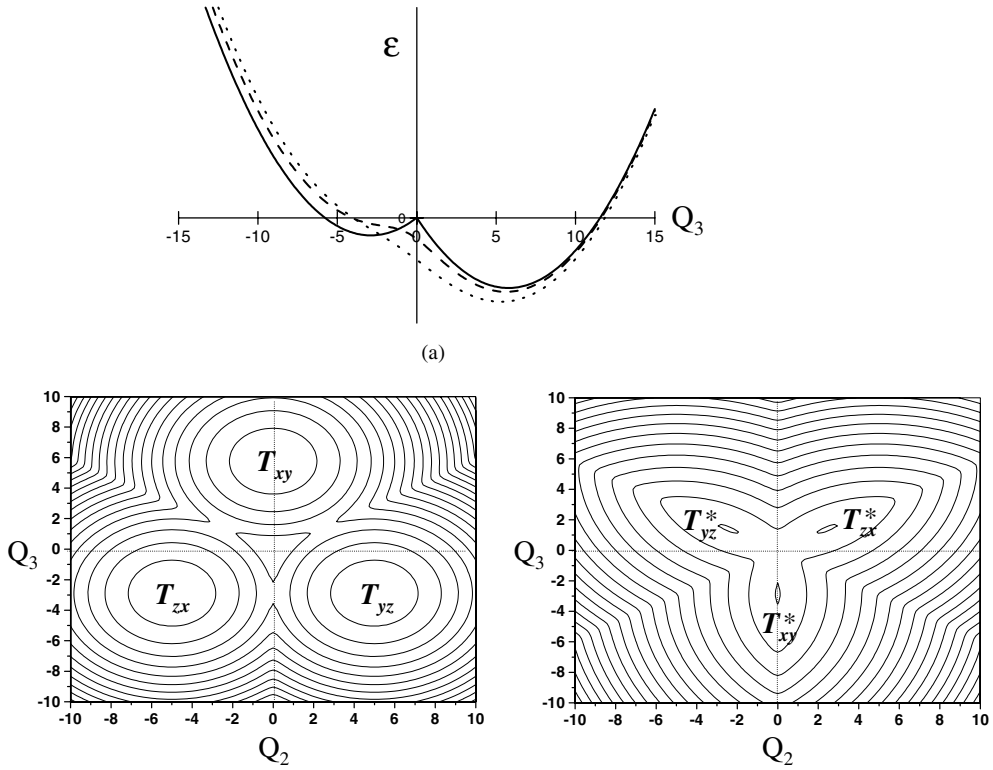

Figure 7. (a) Cross sections of the $^2T_{2g,xy}$ APES along the Q_3 axis. The equation is computed for $K_E = 0.2$, $b = 2$ and several values of g ($= \lambda/b$): $g < 1$ (solid line), $g = 1$ (dashed line) and $g = 2$ (dotted line). (b) Schematic contour map for the locations of the two kinds of minimum: T (left) and T^* (right).

Secondly, we shall discuss the energy-level scheme of the $^2T_{2g}$ states for KCl:Eu^{2+} in the framework of a model in which the JT and SO interactions are the main perturbation and the CCV is an additional perturbation. If the JTE coupling to the E_{2g} mode takes place along the x axis, the two $T_{2g,xy}$ and $T_{2g,zx}$ states are stabilized by the amount of E_{JT}^E, while the $T_{2g,yz}$ state is destabilized by the amount of $2E_{JT}^E$. In other words, the JTE coupling to the E_{2g} mode splits the threefold degenerate state into the twofold degenerate E(xy, zx) state at low energy and the non-degenerate A(yz) state at high-energy. The SO coupling causes the paraboloids of the low-energy E state to interact, and results into two kinds of minimum i.e. (T_{xy}, T_{xy}^*) on the $^2T_{xy}$ paraboloid and (T_{zx}, T_{zx}^*) on the $^2T_{zx}$ paraboloid, as shown in figure 8. In addition, the CCV must be also considered. If the t_{2g} orbital of the Eu^{2+} ion is well localized and the CCV carries an effective negative charge, a CCV in the nn position is more effective than one in the nnn position. Let us assume that Δ is the attraction, $\langle t_{2g}|V|t_{2g}\rangle$, between the electron cloud of the t_{2g} of Eu^{2+} and the V_c^- with an effective negative charge in the nn position. If the vacancy is located along the [101] direction, the $^2T_{zx}$ state is deepened by 2Δ, while the $^2T_{xy}$

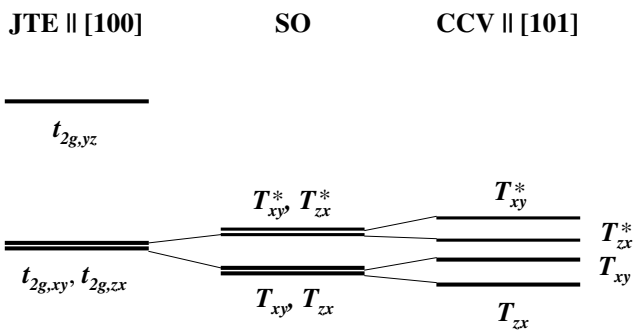

Figure 8. Energy-level scheme of the Eu^{2+} RESs: the Jahn–Teller effect coupling to the E_g mode (left) and the spin–orbit interaction (middle) in the zero-order approximation, and the fine-structure splitting of the lower levels due to the CCV effect located in the nn position.

and $^2T_{yz}$ states are made shallower by Δ. The last column in figure 8 shows the energy-level scheme of the Eu^{2+} RESs, accountable for the observed A-band emission from KCl:Eu^{2+}.

Finally, let us try to understand the features of the polarized A-band emission from KCl:Eu^{2+} on the basis of the RESs, assuming that the polarization of the luminescence is strongly correlated with the nature of the minima on the APES of the excited state. When the crystal is irradiated by the z-polarized light travelling along the x-axis, primarily the $t_{2g}(zx)$ orbital is populated. Then, the T_{zx} and T^*_{zx} minima emit A_Π emission polarized parallel to the direction of the exciting light. Part of the population can arrive at the T_{xy} and T^*_{xy} minima on the $^2T_{xy}$ state via the intersection between the $^2T_{zx}$ and $^2T_{xy}$ paraboloids. Then, the T_{xy} and T^*_{xy} minima emit the A_Σ emission polarized perpendicular to the exciting light. The observed angular dependence of the polarization ratio can be characterized by the symmetry properties of these minima associated with the A-band emission. For the T_{zx} and T^*_{zx} minima, a component of the unit vector of each oscillator is [1 0 1] and [1 0 −1], respectively. According to equation (1), $P(\alpha)$ becomes $\sin(2\alpha)$. Similarly, for the T_{xy} and T^*_{xy} minima, $P(\alpha) = -\cos(2\alpha)$ for the [100]–[010] optical arrangement.

5. Conclusions

The A-band emission from KCl:Eu^{2+}, attributed to the 5d → 4f transition, consists of several Gaussian components. These components may be strongly associated with the complexity in the excited state of the Eu^{2+} ion in KCl. For heavy ions (specially, rare earth ions), it has been argued that the spin–orbit interaction is strong enough to prevent the dynamic Jahn–Teller distortion from occurring. Experimental evidence for the absence of the dynamic Jahn–Teller stabilization can be found in the f → f transitions, in which the bands are very sharp and the Stokes shift is negligible. When the SO is so strong, the qualitative appearance of the threefold $^2T_{2g}$ energy level, reduced from d^1 by the crystal-field potential, is the spin–orbit splitting to a single $|^2T_{2g};\ 1/2\rangle$ at low energy and twofold $|^2T_{2g};\ 3/2\rangle$ at high energy. Furthermore, the JTE coupling with tetragonal and/or trigonal modes may split the doubly degenerate state. For this case, three Gaussian components can be observable in the A → T transition. The characteristic features in the A-band emission are the unusual polarization, multiple components, the strong Stokes shift and the widened band-width. In the $T\otimes E_g$ vibronic approximation, the lower $^2T_{2g}$ state and the upper ^2E_g state cannot mix, so that only the tetragonal minima are reduced on the $^2T_{2g}$ paraboloids. When the spin–orbit coupling is not much stronger than the Jahn–Teller coupling, the off-diagonal element in the SO mixes

the three paraboloids to produce an additional tetragonal minimum on the $^2T_{2g}$ paraboloids. An additional perturbation, the electrostatic effect of the charge compensating cation vacancy on the t_{2g} orbital, is necessary for the fine electronic structure of Eu^{2+} in KCl. Without this model, the observed emission feature cannot be interpreted.

Acknowledgment

The Korean Research Foundation provided a visiting fellowship to support this work.

References

Aguirre de Cárcer I, Cussò F and Jaque F 1988 *Phys. Rev.* B **38** 10 812
Blasse G 1973 *Phys. Status Solidi* b **55** K131
Bron W E and Wagner M 1966 *Phys. Rev.* **145** 689
Choi K-O, Lee S-W, Bae H-K, Jung S-H and Chang C-K 1991 *J. Chem. Phys.* **94** 6420
Fukuda A 1970 *Phys. Rev.* B **1** 4161
Hernandez A J, Murrieta H S, Jaque F and Rubio O 1981 *J. Solid State Commun.* **39** 1061
Kang J-G, Ju S-K, Lee S-W and Kim Y-D 1995 *J. Phys.: Condens. Matter* **7** 7387
Kang J-G, Yoon H-M, Chun G-M, Kim Y-D and Tsuboi T 1994 *J. Phys.: Condens. Matter* **6** 2101
Lawson J K and Payne S A 1993 *Phys. Rev.* B **47** 14 003
Merkle L D and Bandyopadhyay P K 1989 *Phys. Rev.* B **39** 6939
Merkle L D and Powell R C 1977 *Chem. Phys. Lett.* **46** 303
Muñoz G H, de la Cruz C, Muñoz A F and Rubio O J 1988 *J. Mater. Sci. Lett.* **7** 1310
Mugeński E and Nagirnyi V 1994 *Phys. Status Solidi* b **181** K41
Öpik U and Pryce M H L 1957 *Proc. R. Soc.* A **238** 425
Owen J F, Dorain P B and Kobayasi T 1981 *J. Appl. Phys.* **52** 1216
Radhakrishnan J K and Selvasekarapandian S 1994 *J. Phys.: Condens. Matter* **6** 6035
Rubio J O 1991 *J. Phys. Chem. Solids* **52** 101
Sosa R F, Alvarez E R, Camacho M A, Muñoz A F and Rubio J O 1995 *J. Phys.: Condens. Matter* **7** 6561